Metrol. Meas. Syst. Vol. XVI (2009), No 4, pp. 631-640

PAN POLSKA AKADEMIA NAUK

METROLOGY AND MEASUREMENT SYSTEMS

Index 330930, ISSN 0860-8229

www.metrology.pg.gda.pl

M&MS

EXCITATION-INDEPENDENT CONSTANT CONDUCTANCE ISFET DRIVER

Maciej Kokot[1)], Tadeusz Ossowski[2)]

1)Gdansk University of Technology, Faculty of Electronics, Telecommunication and Informatics, G. Narutowicza 11/12, 80-952 Gdańsk, Poland (✉ kokot@ue.eti.pg.gda.pl, +48 58 347 1511)
2)University of Gdansk, Faculty of Chemistry, Sobieskiego 18, 80-952 Gdańsk, Poland (tedos@chem.ug.gda.pl)

Abstract

A new constant conductance driver for ISFETs sensors has been developed. The proposed circuit maintains the sensor operating point at constant drain-source conductance. The combination of a simple, self-balancing resistance bridge and the subtraction of half (or similar fraction) of source-drain voltage from the gate-source voltage provides independence of the output signal from current and voltage drivers instability. The use of precision current sources or high class operating amplifiers is not required. The operating point depends on precision bridge resistors only. The driver presented here simplifies applications of ISFET sensors in battery-powered handheld devices without the accuracy trade-off which the second part of the paper shows.

Keywords: ISFET, constant conductance driver, self-balancing resistance bridge, operating point stability.

1. Introduction

The ISFETs are sensors that provide an electrical signal as the response to the concentration of ions in a solution, mainly hydrogen ions [1]. These sensors provide important advantages compared to the traditional glass electrodes, particularly due to their small size, solid state and faster response [2]. The glass electrode has a great output resistance and a high class input amplifier is required. Fortunately, the output resistance of an ISFET sensor is small [3]. This type of semiconductor sensors has recently gained much popularity [4] due to their small size and fast flow measurement capability [5]. The applicability of ISFETs in environmental water analysis was also evaluated in recent years by the European FP5 Project [6, 7].

The electric circuits used up to now for sensor biasing are simple [1, 8, 9, 10, 11]. Mostly there are source and drain followers (which can be seen as some kind of self-balancing bridge), as shown in Fig. 1.

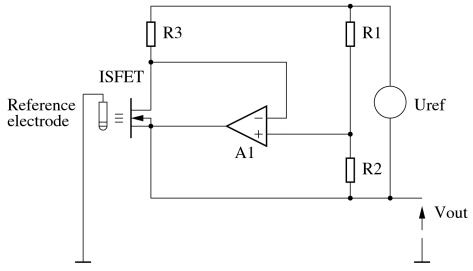

Fig. 1. The basic circuit diagram of a source and drain follower [1].

Article history: received on Jul. 7, 2009; received in revised form on Nov. 23, 2009; accepted on Nov. 27, 2009, available online on Dec. 11, 2009.

The working point of the ISFET's drain-source part is constant (constant current and constant voltage) which eliminates the current-voltage characteristics of a transistor. The gate-source voltage variation is the electrical output signal.

The main disadvantage of traditional circuits is the necessity of very accurate drain current and an independent drain-source voltage control. Instability in voltage or current sources results in a significant output signal change.

The main goal of the present work is to get a polarization circuit small and simple, but independent of current and/or voltage sources accuracy. The evaluation of this circuit's application in battery powered devices will be shown. The preliminary research was presented in [12].

2. Theoretical analysis

The ISFET/MEMFET is in fact nothing else then a MOSFET with the gate separated from the chip in the form of a reference electrode inserted in a solution. An electric charge, which depends of the ion concentration in the solution, is formed on the surface of the gate dielectric [1, 2]. This charge modifies the threshold voltage with almost Nernstian sensitivity of 59 mV per decade of ion (mostly hydrogen) activity (concentration) [1].

$$\Delta V_t = -2.3\frac{RT}{F}\alpha\Delta pH, \tag{1}$$

where R and F are gas and Faraday constants, T is temperature, and α is a dimensionless parameter that varies between 0 and 1, depending on the intrinsic buffer capacity of the dielectric layer [2].

The expression for the threshold voltage of an ISFET is:

$$V_t = V_{t(pH=7.0)} + K\left(pH - 7.0\right), \tag{1a}$$

where $V_{t(pH=7.0)}$ is the threshold voltage in a neutral solution and K is the sensitivity parameter.

The general expression for the drain current of the ISFET in non-saturated mode is the same as for a MOSFET [13]:

$$I_d = \beta\left(\left(V_{gs} - V_t\right)V_{ds} - \frac{1}{2}V_{ds}^2\right) \tag{2}$$

with:

$$\beta = C_{ox}\mu\frac{W}{L} \tag{3}$$

constant for the particular transistor, where C_{ox} is the oxide (gate insulation) capacity per unit area, W and L the width and the length of the channel respectively, and μ is the electron mobility in the channel. V_t is the threshold voltage and depends on ion concentration.

As can be seen from Eqn. 2, keeping the difference between V_{gs} and V_t constant makes I_d constant if V_{ds} is also constant. V_{gs} is the output signal, but it depends not only on V_t but also on I_d and V_{ds} stability provided by an external circuit.

Dividing Eqn. 2 by V_{ds} gives an expression for the drain-source conductance:

$$G_{ds} = \frac{I_d}{V_{ds}} = \beta\left(V_{gs} - V_t - \frac{1}{2}V_{ds}\right). \tag{3}$$

Taking the gate-center of channel voltage as the output signal gives a simpler one:

$$G_{ds} = \beta\left(V_{gc} - V_t\right), \tag{4}$$

where:

$$V_{gc} = V_{gs} - \frac{1}{2}V_{ds}. \tag{5}$$

As can be seen from Eqn. 5, if G_{ds} is kept constant, the output signal V_{gc} depends only on V_t (which depends on the ion concentration) and is independent from I_d or V_{ds}.

It should be stated here that a non-saturated ISFET's mode operation must be assured. Traditional (constant voltage constant current) ISFET bias circuits work correctly also in a saturated point, but at the cost of precision current or voltage sources.

3. Circuit description

The circuit shown in Fig. 2 is formed by a resistance bridge with the ISFET in one arm and the voltage divider P_1 in another arm. Two resistors R_1 and R_2 are equal. The bridge is self-balanced by the operational amplifier A_1 which provides the ISFET's source-drain conductance equal to constant value P_1 by changing the source potential. The potentiometer P_1 divides V_{ds} in a 1:1 ratio which gives on its tap the virtual center-of-channel potential, so $V_{out} = -V_{gc}$. If the tap of P_1 is slid down, the circuit is equal to that in Fig. 1. V_{out} is buffered by a voltage follower with the operational amplifier A_2.

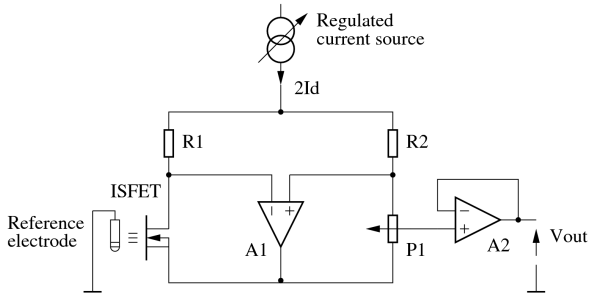

Fig. 2. Constant conductance driver circuit.

The regulated current source $2I_d$ was used only for measurement purposes, the same as the potentiometer P_1. In the final circuit these elements are not necessary.

The electronic components used here are general-purpose elements. Operational amplifiers are OP07C, with low input offset voltage (60 μV) and low input bias current (2 nA) [14]. The resistors are metal film low tolerance (1%) and have a resistance of 2.49 kΩ. The precision potentiometer has a resistance of 1 kΩ. The reference electrode is a non-saturated silver-chloride one.

4. Experimental results

To verify the proposed circuit, a n-type Si_3N_4 depletion mode ISFET [15] made in the Institute of Electron Technology in Warsaw was used in different pH solutions. The operating point of the sensor was fixed to a drain-source resistance equal to 1kΩ.

In Fig. 3 the experimental results for variable drain current obtained with this polarization circuit for different pH solutions can be seen. Solid lines show the $-V_{gc}$ output voltage which can be compared with dotted lines showing the uncompensated $-V_{gs}$ voltage output obtained with the P_1 tap slid down. These results show that the proposed circuit maintains rather good output voltage independence from the drain current in contrast to classical ISFETs'

conditioning circuits (dotted lines), but not totally current independent, as could be expected from Eqn. 4.

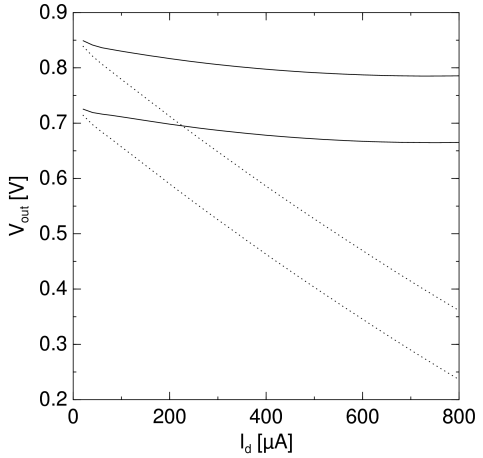

Fig. 3. Experimental results of drain current influence on the output voltage $-V_{gc}$ (solid lines) and $-V_{gs}$ (dotted lines) in constant conductance mode in solutions of pH 4.01 (upper pair) and 7.00 (lower pair).

In the proposed circuit this low dependency can be also compensated. One can slightly change the P_1 1:1 ratio and achieve much better independence from drain current. The additional experimental data are shown in Fig. 4. The solid line shows the data with the P_1 tap at the half position and the other lines with the tap slightly above the center position.

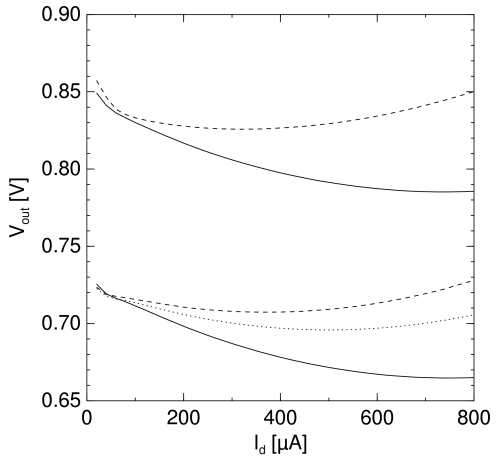

Fig. 4. Compensation of V_{ds} influence in pH 7.00 (lower lines) and 4.01 (upper lines). The P1 ratio is: 1:1 (solid lines), 550:450 (dotted lines) and 575:425 (dashed lines).

5. Discussion

The experimental results are not in full compliance with the theory shown here earlier. The main reason is a generalization of Eqn. 2 which is the first-order approximation of the more accurate expression for the drain current shown below [13]:

$$I_d = \beta\left(\left(V_{gs} - V_t\right)V_{ds} - \frac{1}{2}V_{ds}^2 - \frac{4}{3}\varphi^{1/2}V_{ds}^{3/2} \right), \tag{7}$$

where φ is non-zero potential, which introduces substrate doping influence with V_{ds} in power of 3/2:

$$\varphi = \frac{1}{4}\frac{2e\varepsilon\varepsilon_0 N_a}{C_{ox}^2}, \tag{8}$$

where, most important, N_a is the acceptor concentration in the doped transistor substrate.

Eqn. 5 now has the more accurate form:

$$G_{ds} = \beta\left(V_{gc} - V_t - \frac{4}{3}\varphi^{1/2}V_{ds}^{1/2} \right). \tag{9}$$

As can be seen from Eqn. 9, the output signal V_{gc} is not totally independent from V_{ds} (or I_{ds} also) but this dependency is rather low, especially when the doping level of substrate – N_a is low.

The second-order approximation of the drain current expression is widely used in computer-aided design for increased accuracy[16]:

$$I_d = \beta\left(\left(V_{gs} - V_t\right)V_{ds} - \frac{1+\delta}{2}V_{ds}^2 \right). \tag{10}$$

The 2nd order, medium-accuracy form of Eqn. 5:

$$G_{ds} = \beta\left(V_{gc} - V_t - \frac{\delta}{2}V_{ds} \right). \tag{11}$$

The circuit proposed here can compensate this non-zero δ coefficient with the non-1:1 ratio of P_1. The first- and second-order (Eqn. 2, 5 and 10, 11) approximations of the ISFET models are fully covered by the driver shown here, but the most accurate square-root approximation with the Eqn. 7, 9 is not possible to achieve with the proposed circuit.

6. Model parameters and accuracy estimation

The parameters of drain current expressions (Eqn. 2, 10 and 7) was estimated from the measured data and they are shown in Table 1. The parameter β was extracted from additional measurement, because in the constant-conductance mode it is combined with V_t and it is impossible to extract it separately.

Table 1. The ISFET model parameters.

Model	Equation	β	Vt(pH=4.01)	Vt(pH=7.00)	δ	φ
		[mA/V^2]	[V]	[V]	[-]	[V$^{1/2}$]
1st	**2, 5**	1.93	-1.309	-1.186		
2nd	**10, 11**	1.93	-1.353	-1.231	0.216	
3rd	**7, 9**	1.93	-1.384	-1.263		0.0088

The ISFET pH sensitivity factor K (Eqn. 1a) has the same value of 41mV/pH for all approximations and real measurements. The differences of V_t in various models are only due to the best-fit approximations in the wide drain current region.

The circuit's $-V_{gc}(I_d)$ response with the three models of ISFET transistor was simulated. The differences between the simulated and measured $-V_{gc}$ are shown in Fig. 5. The solid line is the approximation error with ISFET first-order model given by Eqn. 2. It is also the measurement error of the circuit with P_1 ratio of 1:1. The dotted line is the error with second-order Eqn. 10 taken and measurement error with P_1 in $(1+\delta)$:$(1-\delta)$ ratio. The third, dashed line is the Eqn. 7 transistor model approximation error.

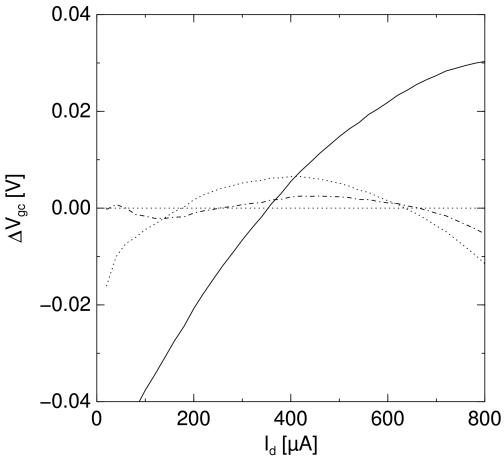

Fig. 5. Approximation errors of various ISFET models. The solid, dotted and dashed lines show differences between measured and simulated $-V_{gc}$ with 1st, 2nd and 3rd order models respectively.

The best approximation is achieved with the nonlinear 3rd order model, but the 2nd order (achievable with the presented driver) is not significantly worse, especially with not-so-great drain current variations.

7. Application of the proposed circuit in a battery powered pH-meter

The goal of this paper was also to show the potential applications of the proposed sensor circuit. The independence of the bridge current simplifies the battery-powered meter construction.

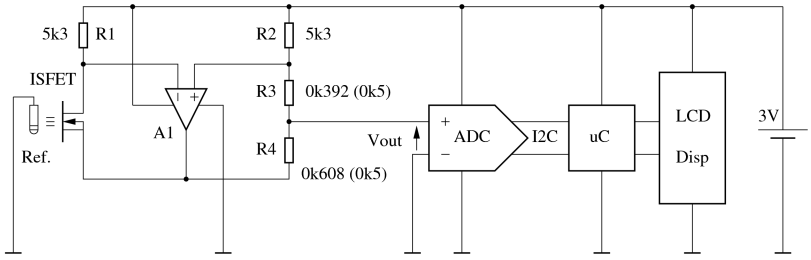

Fig. 6. The battery-powered pH-meter.

As the main power source a lithium 3 V battery was selected and the circuit is powered directly from it. An ISFET's 0.4 mA drain current was chosen. The circuit of the device is shown in Fig. 6. A low-power 8-bit micro-controller with LCD display and the MCP3421 18-bit sigma-delta analog-digital converter with internal reference voltage was used. The rail-to-

rail operational amplifier MCP6V01 provides the bridge self-balance. All electronic components can operate properly with the said battery power [17].

The main source of this pH-meter's inaccuracy is battery voltage instability: from 3.3 V (when fresh) to 2.7 V (at end-of-life) which results in bridge current variations. But pH changes also contribute to bridge current variations.

The 3rd order ISFET model and its parameters from Table 1 were used in the simulation of the pH-meter response to the various pH values and battery voltages.

In Fig. 7 the simulated responses of the proposed pH-meter in a wide pH range with the battery voltage equal to 3.0 V on the left side and the magnified part for various battery voltages on the right side are shown. The dotted line is the output voltage for $R_3=R_4=0.5$ kΩ (which gives the 1st order accuracy of the ISFET driver), the solid line is for $R_3=(1-\delta)0.5$ kΩ, $R_4=(1+\delta)0.5$ kΩ (the 2nd order accuracy).

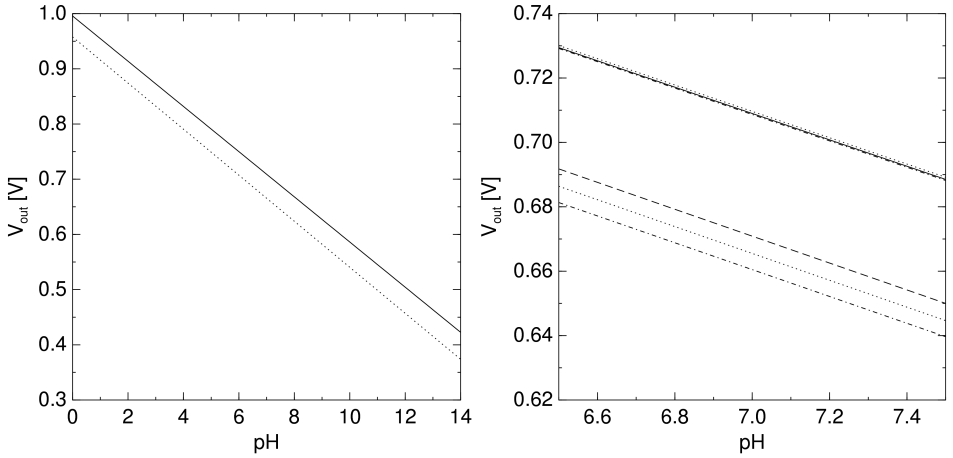

Fig. 7. The output voltage of the pH-meter. The solid line is with the δ compensation and the dotted – without. Battery voltage is 3.0 V for the left side and 2.7, 3.0 and 3.3 V for the right.

The drain current varied from 0.35 mA at pH=0 to 0.45 mA at pH=14 with the battery voltage 3.0 V. In the worst case, the variations were from 0.30 mA at pH=0 and V_{Batt}=2.7 V to 0.50 mA at pH=14 and V_{Batt}=3.3 V.

The linear regression coefficients of the Fig. 7 data were extracted and are shown in Table 2.

Table 2. The linear regression coefficients.

V_{BATT}	1st order (δ=0)				2nd order (δ=0.216)			
	V_{out}=f(pH)		pH=f(V_{out})		V_{out}=f(pH)		pH=f(V_{out})	
	A	B	a=1/A	b=-B/A	A	B	a=1/A	b=-B/A
[V]	[V/pH]	[V]	[pH/V]	[pH]	[V/pH]	[V]	[pH/V]	[pH]
2.7	-0.0417	0.9628	-23.974	23.082	-0.0409	0.9951	-24.429	24.309
3.0	-0.0417	0.9575	-23.974	22.955	-0.0409	0.9956	-24.429	24.321
3.3	-0.0417	0.9523	-23.974	22.830	-0.0409	0.9960	-24.429	24.331

The 1st and 2nd order versions of the pH-meter were virtually calibrated with linear regression coefficients from Table 2 with the battery voltage equal to 3.0 V. The output

voltage errors were shown in Fig. 8 for both non- and δ-compensating variations, where a 6mV output voltage error corresponds with a 0.15 pH measurement error.

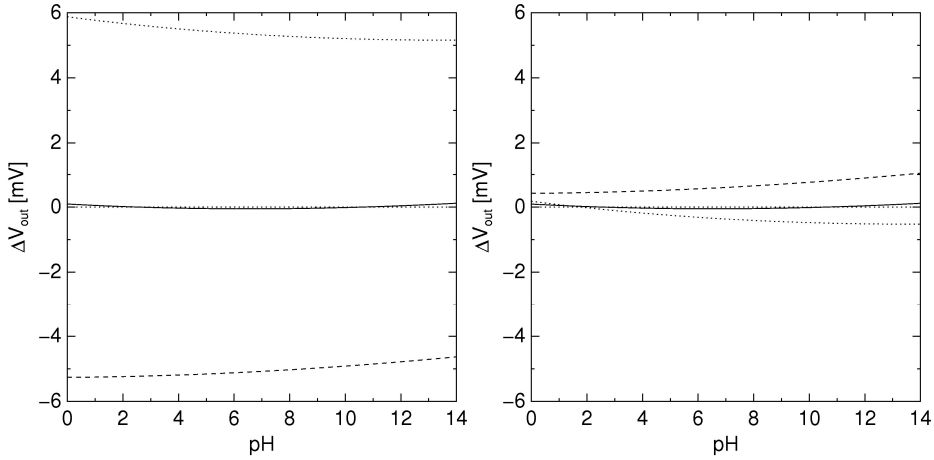

Fig. 8. The pH-meter measurement errors without δ-compensations (R3=R4) – left and with δ-compensation – right, at battery voltages: 3.0 V (solid lines), 2.7 V (dotted) and 3.3 V (dashed).

With the mean-life 3.0 V battery voltage these errors are insignificant. But with a fresh or at the end-of-life-state battery they are much (without δ coefficient compensation) and slightly (with compensation) more visible. The overall errors are in the range of ±0.15 pH and in the range of ±0.025 pH respectively.

8. Conclusions

This paper presents a new conditioning circuit for ISFET sensors. The great advantages of this circuit are its accuracy and stability which depend only on the bridge resistors. No precise current or voltage sources are needed. The output signal is almost independent of the bridge supply despite the change of the operating point of the ISFET. The driver circuit approximating the 1st order transistor model did not give the suspected wide-supply-change accuracy, but the 2nd order model (with the non-1:1 drain-source divider) achieved very good precision.

The potential applicability of the proposed sensor circuit in simple but precision battery-powered pH-meters was also shown. The accuracy of the said meter was estimated, and also a comparison between the 2nd order – δ-compensating and the 1st order – non-δ-compensating circuits was made. With the former, the measurement error is in the range of 0.025 pH error in the full range of pH and battery voltage, which is comparable with high-grade laboratory pH-meters.

References

[1] P. Bergveld: “Thirty years of ISFETOLOGY”. *Sens. Actuators, B, Chem.*, vol. 88, 2003, pp. 1-20.

[2] P. Bergveld: “ISFET, Theory and Practice”. *IEEE Sensor Conference*, Toronto 2003.

[3] M. Yuqing, C. Jinrong, F. Keming: “New technology for the detection of pH”. *J. Biochem. Biophys. Methods*, vol. 63, 2005, pp.1-9.

[4] A. Dybko: “Chemical sensors metrology”. *Metrol. Meas. Syst.*, vol. 8, no. 4, 2001, pp. 357-365.

[5] A. Dybko: "Automated measuring system for testing chemical sensors". *Metrol. Meas. Syst.*, vol. 8, no. 3, 2001, pp. 263-270.

[6] M. Chudy, W. Wróblewski, A. Dybko, Z. Brzózka: "Natural Water Analysis Based on Multisensor System". *MIXDES Conference*, Wrocław, Poland 2002.

[7] J. Ogrodzki, L.J. Opalski: "Modeling of semiconductor ion sensors for CAD". *Proceedings of 6th MIXDES*, Gdynia, Poland, 2000, pp. 253-257.

[8] S. Casans, A.E. Navarro, D. Ramirez *et al*.: "Novel constant current driver for ISFET/MEMFETs characterization". *Sens. Actuators, B, Chem.*, vol. 76, 2001, pp. 629-633.

[9] S. Casans, A.E. Navarro, D. Ramirez *et al*.: "Novel voltage-controlled conditioning circuit applied to the ISFETs temporary drift and thermal dependency". *Sens. Actuators, B, Chem.*, vol. 91, 2003, pp. 11-16.

[10] B. Palan *et al.*: "New ISFET sensor interface circuit for biomedical applications". *Sens. Actuators, B, Chem.*, vol. 57, 1999, pp. 63-68.

[11] W. Chung, C. Yang, D. Pijanowska, A. Krzyskow, W. Torbicz: "ISFET interface circuit embedded with noise rejection capability". *Electronics Letters*, vol. 40, no. 18, 2004, pp. 1115-1116.

[12] M. Kokot, T. Ossowski: "Constant conductance driver for ISFET". *PAK*, vol. 54, no. 3, 2008, pp. 145-147. (in Polish)

[13] J. Huang, G. Taylor: "Modeling of an ion-implanted silicon-gate depletion-mode IGFET". *Electron Devices, IEEE Transactions on*, vol. 22, 1975, pp. 995-1001.

[14] Ultralow Offset Voltage Operational Amplifier OP07. Datasheet from Analog Devices. Online: *http://www.analog.com/static/imported-files/data_sheets/OP07.pdf* [as of July 6, 2009].

[15] B. Jaroszewicz, P. Grabiec, J. Koszur, A. Kosiubiński, Z. Brzózka: "Technology and Measurements of Backside Contacted ISFETs". *MIXDES Conference*, Wrocław 2002.

[16] G. Merckel, J. Borel, N. Cupcea: "An accurate large-signal MOS transistor model for use in computer-aided design". *IEEE Transactions on*, vol. 19, 1972, pp. 681-690.

[17] Datasheets from Microchip. Online: *http://www.microchip.com* [as of September 3, 2009].